S-Band Smallsat InSAR Constellation for Surface Deformation Science

Anthony Freeman
Jet Propulsion Laboratory
California Institute of Technology
Pasadena, CA, USA
anthony.freeman@jpl.nasa.gov

Nacer Chahat
Jet Propulsion Laboratory
California Institute of Technology
Pasadena, CA, USA

***Abstract*—Surface deformation studies using repeat-pass interferometric SAR have evolved into a powerful tool for geophysicists studying earthquake fault zones, volcanoes, ice sheet motion, and subterranean aquifers. Longer wavelengths (S-Band and L-Band) are preferred because they do not decorrelate as quickly as shorter wavelengths. Rapid revisit (1-3 days) is preferred because it allows the study of these phenomena at the timescales at which they commonly occur. Global access on such timescales is also required. Vector surface deformation measurements, taken from more than one direction, are a desired feature.**

This paper describes the architecture of a longer wavelength, Smallsat SAR constellation of up to 12 satellites for rapid revisit surface deformation studies. The key to making such a constellation affordable is to lower launch costs, spacecraft costs, and instrument (SAR) costs. The first two objectives can be achieved using an ESPA-ring compatible, Smallsat spacecraft. The third objective requires a SAR instrument sized to fit the mass and volume constraints imposed by such a spacecraft. Current state-of-the-art in miniaturization of electronics means that the radar transmit, receive and data handling functions can easily be implemented in a compact, single-string, low mass solution. The most significant challenge in designing a SAR to fit the Smallsat paradigm is in the dimensions of the antenna.

The antenna sizing problem is addressed by adopting a smaller antenna than allowed by conventional SAR design rules. The antenna design is simple, requiring no electronic beam-steering or beam-forming capability. Both reflectarray and microstrip patch antenna solutions are considered. The antenna structure is dual-purpose, to limit the overall system mass, with solar panels on the backplane providing power for the radar and spacecraft. The proposed solution easily accommodates radar squint angles of +/- 30 degrees for repeat-pass interferometry measurements from multiple directions.

Keywords—Synthetic Aperture Radar, Repeat-pass interferometry, surface deformation, Smallsat

I. INTRODUCTION

Repeat-pass Interferometric SAR [1], also known as InSAR, is by now a well-established tool in the arsenal of Earth scientists, who use it to study surface deformation in geophysically active areas, such as along earthquake faults, in volcanic regions, subsurface aquifers, and the major ice sheets. A long-standing goal of this community [2] has been to field a constellation of InSAR satellites, producing deformation maps in geophysically active areas at up to daily intervals, with full vector displacements at submillimeter per year accuracies. The joint NASA/ISRO SAR mission [3], known as NISAR, and currently planned for launch in 2020, is a significant step on the road to this future capability, with systematic, global access on a 12-day revisit interval.

NISAR is a wide-swath (~250 km), medium spatial resolution (~10m) mapping system that provides both L-Band and S-Band InSAR measurements to achieve the mission objectives. Simultaneous wide swath and spatial resolution capability is achieved using the SweepSAR technique [4], a form of scan-on-receive beamforming that uses a large (12m diameter), passive reflector combined with a phased array feed. The requirements expressed in [3] could be met with a constellation of four NISARs, spaced out in separate orbits, according to one of the leading scientists in the Solid Earth science community [5]. The NISAR flight system is a medium to large-class spacecraft, so a 4-element constellation would be very expensive for NASA to undertake on its own – a lower-cost alternative could, therefore, prove to be attractive.

In this paper, an architecture is presented for a low-cost S-band InSAR constellation, with a capability that matches a constellation of four NISAR platforms at the same wavelength.

In section II, the factors driving the mission design for the constellation are described. Section III illustrates a novel approach to SAR design, in which the SAR antenna is deliberately sized to be smaller than convention would allow. This builds on work previously published by one of the authors in references [6] and [7]. In section IV two design approaches are summarized or the SAR antenna that are currently under study – a microstrip patch antenna array, and a reflectarray solution. In both cases the backplane of the antenna is populated with solar panels to provide power for radar operations, similar to the ISARA flight demonstration [8].

II. MISSION DESIGN

A. Orbit selection

The preferred orbit for the constellation is sun-synchronous, circular and near-polar at an altitude of around 600 km. This orbit provides global access, at the lowest possible altitude for radar operation, with acceptable drag

levels to reduce orbit maintenance operations. It is assumed that a constellation of 12 satellites, spaced at one-day intervals, in a 12-day exact repeat orbit, will provide the required temporal revisit frequency.

B. Launch Strategy

Specifying an ESPA-ring compatible spacecraft, with dimensions 1.0x0.7x0.6 m, and mass < 180 kg, allows one to take advantage of low-cost secondary launch opportunities on ESPA ring slots [9]. This enables up to six elements of the InSAR constellation to be launched at a time. After launch, individual elements of the constellation will have to be phased into their required orbits, using a propulsion system, also needed for orbit maintenance. ESPA-ring spacecraft are also compatible with the Venture-class, low-cost small launch vehicles that NASA is currently sponsoring [10], expanding the range of launch options available for the constellation. This flexibility in launch options allows for redundancy at the flight system level throgh simple replenishment of the constellation in the event an element fails and as they age and are retired.

C. Spacecraft Selection

Several spacecraft manufacturers based in the US offer suitably inexpensive, ESPA-ring compatible Smallsats.

D. Concept of Operations

After launch, and orbit phasing, InSAR constellation elements will be uploaded commands for operations spanning up to a week. In the event of, for example, a large magnitude earthquake, commands may be updated more frequently. InSAR data will be collected over geophysically active areas on land. Each element can collect data for up to 30 mins per orbit, allowing coverage over the entire land surface. The nominal orientation for data collection has the radar line-of-sight perpendicular, or broadside, to the orbit track. Vector deformation measurements can be collected at squint angles forward and back from this look direction, requiring a trade-off against temporal coverage. Data will be downlinked at X-band using high-latitude ground receiving stations.

III. RADAR DESIGN

A. Wavelength selection

Of the frequencies available for Earth observation using radar, S-Band is selected for the following reasons:

- Longer decorrelation times than for shorter wavelengths
- Less severe ionospheric effects than at L-Band
- Antennas are generally smaller than at L-Band

B. Antenna dimensions

The longest dimension for an ESPA-ring Smallsat is 1 meter. This sets one dimension of the antenna, which therefore cannot be greater than 1 meter, which determines the antenna height dimension, W. Over typical incidence angles, in the range 25 to 35 degrees, a radar antenna of this height, at an altitude of ~600 km, will illuminate a swath of roughly 80 km in the cross-track direction (assuming broadside pointing). The other dimension, the antenna length L, will be set at the shortest for which reasonable InSAR performance can be achieved. For this study L is set at 5 meters.

C. Selecting the PRF

In an earlier paper [6] one of the authors examined the conventional SAR antenna area constraint, showing that it was actually a 'soft' constraint, in that SAR systems can be designed and have been operated with antennas smaller than this constraint would normally allow. This design rule in fact only applies when the SAR system engineer seeks to achieve maximum swath width and minimum possible azimuth resolution at the same time.

It follows from [6] that one can design SARs with PRF's smaller than the Doppler bandwidth provided it is possible to relax the spatial resolution and/or swath width. This result was reported in [7] and is illustrated in Figure 1, in which the Signal-to-Azimuth Ambiguity ratio in dB is plotted for a range of PRF's smaller than the Doppler bandwidth, against the fraction of the available bandwidth used in processing. In [7] the case when the PRF is set at 70% of the Doppler bandwidth B_D was examined; here the PRF is set at 85% of B_D. Figure 1 shows that reasonable azimuth ambiguity levels < -23 dB can still be obtained if only 40% of the available bandwidth is used in SAR processing (azimuth compression). This means that the best achievable azimuth or along-track resolution is now no longer the well-known L/2 limit of conventional SAR design, but it is degraded by a factor (0.85*0.4)=0.34. For the case where L=5m, the best achievable azimuth resolution is now, therefore, ~7.5m. Note that this still consistent with the NISAR medium spatial resolution requirement of 10 m.

Two other well-known limits on the PRF from [6] place upper bounds on its value. The first (PRF upper limit 1) says that to avoid significant range ambiguities the PRF must be smaller than the time it takes to collect returns from the *recorded* swath on the ground. The second (PRF upper limit 2) says that the PRF must be smaller than the time it takes to collect returns from the *illuminated* swath on the ground. Generally the recorded swath is smaller than the illuminated swath, so PRF lower limit 2 is more stringent.

Figure 2 shows the PRF upper and lower limits for the S-band case under study, with the PRF selected for nominal broadside operation indicated on the figure. Also shown is the

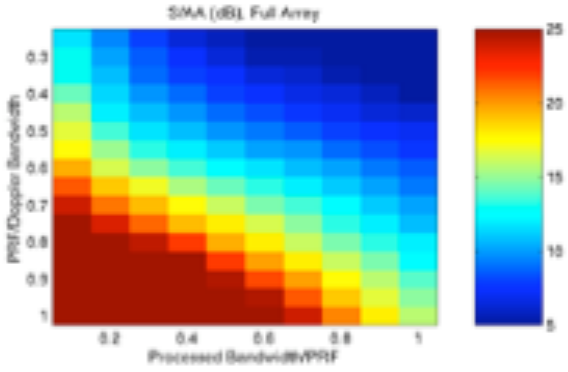

Fig. 1. Signal-to-Azimuth Ambiguity ratios in dB as a function of the PRF expressed as a fraction of the Doppler Bandwidth and the Processed Bandwidth expressed as a fraction of the PRF. Signal and ambiguity levels were integrated over the available processing bandwidth to generate these results. A planar array with side-looking (broadside) geometry was assumed.

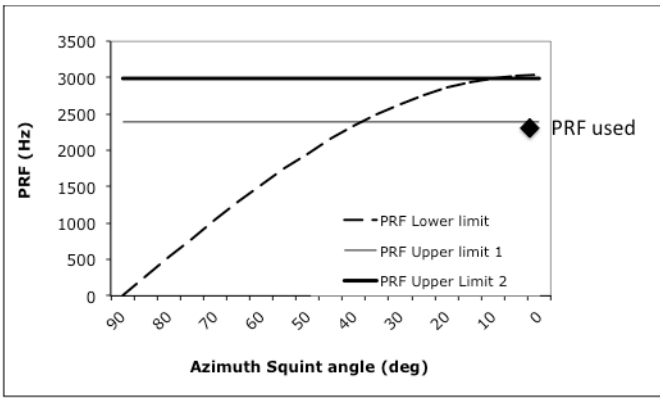

Fig. 2. PRF upper and lower limits for the S-Band SAR example. The PRF value used in the design is indicated. The lower limit on the PRF for a conventional SAR, which depends on the Doppler bandwidth, is shown to vary with squint angle, whereas the two upper limits do not.

variability of the Doppler bandwidth as a function of squint angle, which was also explored in [7]. Basically, B_D falls off as the antenna is squinted off-broadside. For example, at +/- 30-degree squint angles, this means that the selected PRF and the 'lower limit' are closer in line, allowing better azimuth resolution than the broadside case, or more looks in azimuth.

Operating at squint angles +/- 30 degrees off broadside can fulfill the requirement expressed in [3] for vector surface deformation measurements. The trade-offs are that the swath width for off-broadside squint angles will be narrower (by about 30%), and the point spread functions in the SAR image will not be orthogonal. The latter may not matter in InSAR analysis for geophysical applciations, for which the measurement of importance is the relative phase between acquisitions: conventional SAR image quality is less important.

D. Signal-to-noise

The rest of the SAR design uses the conventional radar equation [11] to define the peak RF power, the transmit pulse length, and the noise-equivalent sigma-zero. An RF amplifier with 40% efficency is assumed in estimating the DC power consumption when the radar is transmitting.

E. Data rate

The raw data rate produced by the SAR when operating is also estimated using conventional methods [11], which depend primarily on the bandwidth of the transmitted pulse, B_p and the swath width covered. B_p is set at 25 MHz to provide 10 m ground range resolution at the range of incidcnce angles adopted for this design. (8:4) bit Block Floating Point Quantization is assumed, and an azimuth prefilter of (3:1) is applied to reduce the data rate to reasonable levels. The azimuth prefilter, applied in the frequency domain, notches out only the one-third of the Doppler bandwidth that is used in azimuth compression.

F. SAR performance

The performance of the S-Band SAR design is summarized in Table 1. Note the low on-orbit DC power required to operate the radar, at just 54 W in total, the estimated mass of the single-string radar electronics is 25 kg, and the low data rate, which is just 65 Mbps. Each of these numbers are sized to fit the power, payload mass and data handling capacity of a typical Smallsat spacecraft platform.

TABLE I. S-BAND SAR POINT DESIGN PARAMETERS

Parameter	***Value***
Orbit altitude	600 km
Center frequency	3.2 GHz
Incidence angles	25 – 35 degrees
Squint angle (relative to broadside)	0 degrees
Transmit Peak RF Power	500 W
DC Power when radar is on	180 W
On-orbit average DC power	54 W
Radar electronics mass (single-string)	25 kg
Pulse length	50 μs
Antenna dimensions (L X W)	5.0 X 1.0 m
F/D ratio (for reflectarray)	0.5
Bandwidth	25 MHz
Data rate (3:1 presum, 8:4 BFPQ)	65 Mbps
On-time per orbit	20-30 mins
Downlink rate	300 Mbps
Noise-equivalent sigma-zero	-19 dB
Spatial resolution/ [# of looks]	10 m/ [1]
Swath width	80 km

IV. ANTENNA OPTIONS

The selected antenna architecture is a single-polarization planar array, deployable in one dimension. It is passive, in that no electronic beam steering or beam forming is required. The bandwidth is less than 1% of the center frequency, making the design challenge simpler. Table 2 summarizes desired characteristics for the 5 X 1 m SAR antenna array.

Two approaches for the antenna design are considered: a center-fed microstrip patch array, and an offset-fed reflectarray. Both are shown conceptually in Figure 3. Both antenna arrays are stowed to fit in the ESPA-ring volume constraint. The reflectarray architecture is more complex, requiring the additional deployment of a secondary reflector on an extendable boom, as shown in the figure.

TABLE II. DESIRED ANTENNA CHARACTERISTICS

Parameter	***Value***
Polarization	Single, HH
Center frequency	3.2 GHz
Bandwidth	25 MHz
Maximum Possible Boresight Gain	38.5 dB
Flatness requirement after deployment (λ/10)	9 mm

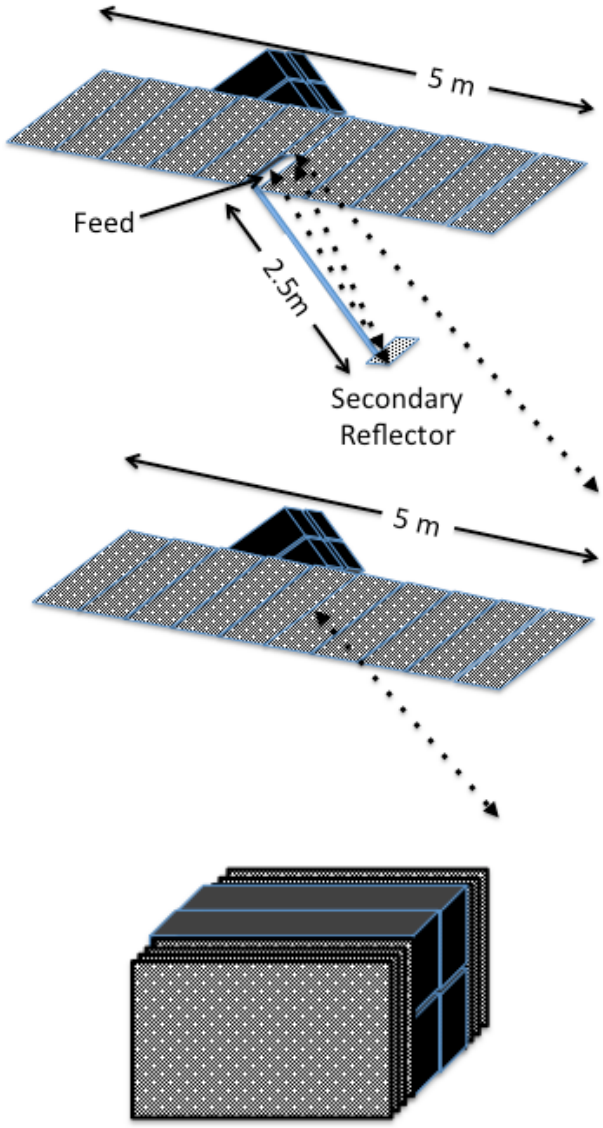

Fig. 3. S-Band SAR flight system concepts with reflectarray (top) and microstrip patch (center) antennas. Both are shown in stowed configuration in the cartoon at the bottom.

Figure 4 shows the conceptual design of the feed for a 3-panel (3 X 1 meter) microstrip patch antenna – extending this to a 5-panel antenna is relatively straightforward. The feed cabling and attachments will not take up all of the real estate on the antenna backplane, leaving room for the placement of solar panels. This approach, combining solar array panels with an RF antenna, is being flight-tested on the ISARA cubesat [8].

V. SUMMARY

A novel architecture for an S-Band InSAR constellation has been presented. A 12-satellite constellation following this architecture should be relatively inexpensive to field – roughly equivalent to the cost of a single NISAR flight system, including launch. This constellation should satisfy a long-standing need of the Earth science community for frequent observations of surface deformation phenomena.

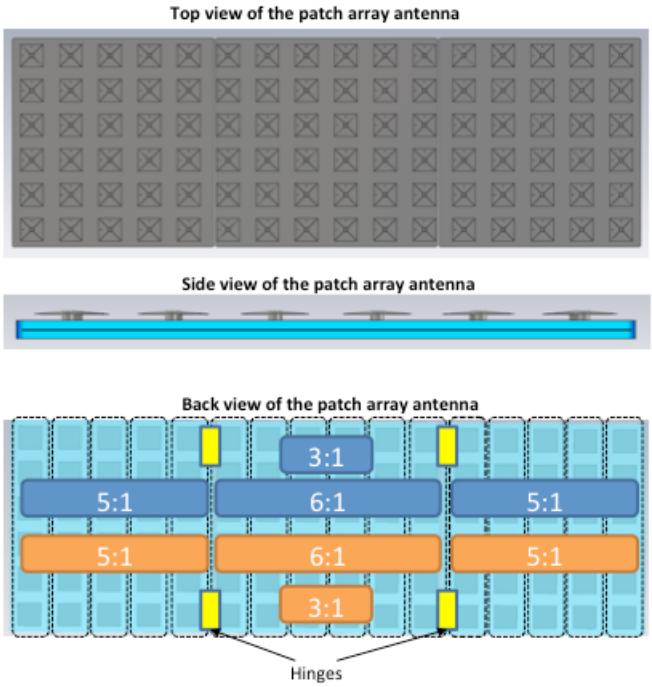

Fig. 4. Conceptual design for a 3-panel microstrip patch array antenna.

ACKNOWLEDGMENTS

The research described in this paper was carried out by the Jet Propulsion Laboratory, California Institute of Technology, under a contract with the National Aeronautics and Space Administration. The authors would like to thank our colleagues at Caltech and JPL who stimulated the discussion that led to this architectural solution, including Charles Elachi, Paul Rosen, Mark Simons, Yunjin Kim, and Jason Hyon; and Tom Cwik for his support of the antenna design work.

REFERENCES

[1] Rosen, P.A., et al., 2000. Synthetic aperture radar interferometry,Proc. IEEE, Vol. 88, No. 3, March 2000, 333–382.

[2] Living on a Restless Planet, NASA Solid Earth Sceince Working Group, 2002, available at http://solidearth.jpl.nasa.gov/PAGES/report.html

[3] http://nisar.jpl.nasa.gov/

[4] Freeman, A., G. Krieger, P. Rosen, Younis, M., W. T. K. Johnson, Huber, S., R. Jordan, and Moreira, A., SweepSAR: Beam-forming on Receive using a Reflector-Phased Array Feed Combination for Spaceborne SAR, Proc. Radarcon '09, Pasadena, CA, May 2009.

[5] Prof. Mark Simons, Caltech, personal communication, 2016.

[6] A. Freeman, W. T. K. Johnson, B. Honeycutt, R. Jordan, S. Hensley, P. Siqueria, and J. Curlander, "The myth of the minimum SAR antenna area constraint," IEEE Trans. Geosci. Remote Sensing, vol. 38, pp. 320–324, Jan. 2000.

[7] Freeman, A., On Ambiguities in SAR Design, Proc. EUSAR 2006, Dresden, Germany, June 2006.

[8] Hodges, R., Shah, B., Muthulingham, D., and Freeman, A., ISARA – Integrated Solar Array and Reflectarray Mission Overview, Annual AIAA/USU Conference on Small Satellites, August 2013

[9] http://www.nasa.gov/press-release/nasa-awards-venture-class-launch-services-contracts-for-cubesat-satellites/

[10] http://www.csaengineering.com/products-services/espa/

[11] SAR Systems and Processing, Curlander, J.C. and McDonough, R. N., publ. J. Wiley, 1991.